ACS Photonics

Article

pubs.acs.org/journal/apchd5

Optimization and Experimental Demonstration of Plasmonic Enhanced Internal Photoemission Silicon Schottky Detectors in the Mid-IR

Meir Grajower,[†] Boris Desiatov,[†] Noa Mazurski,[†] Joseph Shappir,[†] Jacob B. Khurgin,[‡] and Uriel Levy*[,†]

[†]Department of Applied Physics, The Benin School of Engineering and Computer Science, The Hebrew University of Jerusalem, Jerusalem, 91904, Israel

[‡]Department of Electrical and Computer Engineering, Johns Hopkins University, Baltimore, Maryland 21218, United States

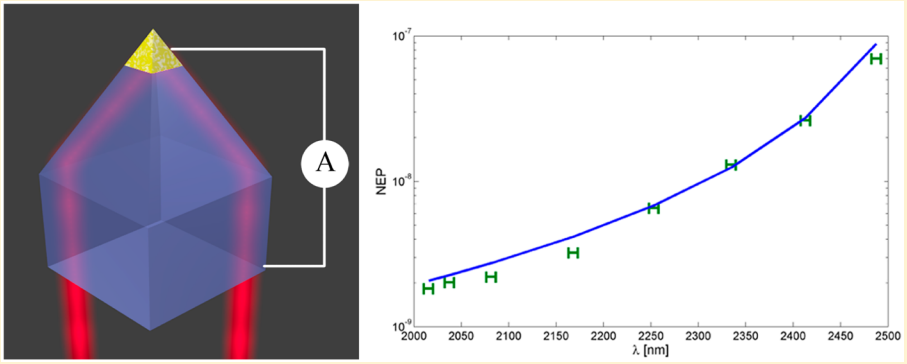

ABSTRACT: Plasmonic enhanced Schottky photodetectors operating on the basis of the internal photoemission process are becoming an alternative for the more conventional photodetectors based on interband transitions for light detection in the infrared. This is because such detectors typically consist of silicon and CMOS compatible metals, thus, allowing low cost and large scale fabrication. Most of the reports so far were focused on measuring the responsivity of the device. Here, we provide a detailed analysis for the optimization of internal photoemission based devices in terms of figure of merits such as signal-to-noise ratio (SNR) and noise equivalent power (NEP). Following the analysis, we experimentally demonstrate the operation of pyramidally shaped, silicon-based, internal photoemission detectors in the mid-infrared. The measured devices are capable of photodetection at wavelengths up to ~2.5 μm. This paves the way for the use of plasmonic enhanced silicon photodetectors for a broad range of applications including mid-IR circuitry and biochemical sensing.

KEYWORDS: *mid-IR, Schotky detector, plasmonics*

Conventionally, detection of light in the visible spectral band is achieved using silicon-based photodetector. The use of CMOS compatible materials and fabrication processes allows to achieve low cost, high yield and large pixel count charge coupled device (CCD) and CMOS-based imagers. Yet, while silicon is the preferred material of choice from these aspects, its interband absorption becomes negligible at wavelengths above ~1.1 μm as the photon energy becomes lower compared with the bandgap of silicon. As such, most of the high quality photodetectors beyond this wavelength are implemented by the use of other materials and concepts.[1,2] For example, telecom-based photodetectors are typically implemented with InGaAs material platform,[2] having a spectral response that can be extended even beyond 2 μm wavelength.[3] The photodetection in other spectral regions, for example, 3−5 μm, is commonly based on InSb,[4−6] whereas in the 8−12 μm regime, the common choice is to use the bolometric approach and HgCdTe (MCT).[5−7]

While these approaches are well-established, such material platforms lack the compatibility with silicon fabrication processes. Therefore, there is a long lasting effort to extend the use of CMOS compatible photodetectors toward longer wavelengths using different materials.[8,9] This effort has been flourishing recently, with the latest achievements in plasmonic enhanced photodetectors based on the internal photoemission (IPE) processes.[10−19] With such an approach, detection of light around 1.3 and 1.5 μm has been achieved, albeit with responsivity significantly lower than the commercial InGaAs-based photodetectors. This is primarily because of the momentum mismatch of electron wave functions in the silicon and the metal. Indeed, it is well-known that the responsivity of IPE-based photodetectors goes down with the increase in the photon wavelength.[19−21] Furthermore, while most of the

Received: February 6, 2017
Published: March 23, 2017

DOI: 10.1021/acsphotonics.7b00110
ACS Photonics 2017, 4, 1015−1020

reports so far are typically geared toward measuring the device responsivity, other important figures of merits such as signal-to-noise ratio (SNR) and noise equivalent power (NEP) are typically ignored.

Hereby, we discuss the optimization of IPE-based photodetectors in terms SNR and NEP. Specifically, we analyze the various noise sources and provide a route toward the optimization of the Schottky barrier for the desired wavelength of operation, depending on the specific operation conditions (e.g., the shunt resistance). Following, we experimentally demonstrate the photodetection of light at wavelengths up to ~2.5 μm by the use of the IPE process in a silicon plasmonic photodetector. The approach is based on achieving plasmonic enhanced IPE in pyramid-like structures acting as an antenna having a large collection cross section of light owing to its relatively large pyramid base and focus it down to the nanoscale apex of the pyramid. This structure already proved itself as a useful solution for the near-infrared (IR) regime.[15] By doing so, the signal is enhanced while the noise is maintained at a low level owing to the small dimensions of the active Schottky junction area. As such, the signal-to-noise ratio (SNR), which is a major limiting factor at these wavelengths is greatly enhanced. The combination of strong light confinement, together with an optimal choice of the Schottky barrier allows achieving mid-IR detection using CMOS compatible materials.

Optimization of Schottky Barrier. We start by discussing the optimization of the Schottky barrier with respect to the desired wavelength of operation. Our figure of merit to be optimized is the signal-to-noise ratio (SNR) defined as

$$\mathrm{SNR} = \frac{\overline{i_{\mathrm{signal}}^2}}{\overline{i_{\mathrm{noise}}^2}} \tag{1}$$

where i_{signal} and i_{noise} are the signal and noise currents, respectively.

The signal current is defined as

$$i_{\mathrm{signal}} = \frac{eP_{\mathrm{in}}}{h\nu}\eta = \frac{P_{\mathrm{in}}}{h\nu}eC\frac{(h\nu - \phi_{\mathrm{B}})^2}{h\nu} \tag{2}$$

where P_{in} is the optical power, e is the electron charge, h is Planck constant, ν is the optical frequency, and η is the quantum efficiency (QE). Using the Fowler model,[20] $\eta = C\frac{(h\nu - \phi_{\mathrm{B}})^2}{h\nu}$, where C is a constant and ϕ_{B} is the Schottky barrier.

There are several noise mechanisms to be considered in our system:[22]

1. Background noise: the background noise can be calculated according to $2e(Q_{\mathrm{B}}\eta e)\Delta\nu$, where Q_{B} is the number of background photons in the spectral bandwidth and $\Delta\nu$ is the bandwidth of photodetection.
2. Johnson noise: the Johnson noise can be calculated according to $\frac{4kT}{R_{\mathrm{L}}}\Delta\nu$, where k is the Boltzmann's constant, T is the temperature, and R_{L} is the load resistance.
3. Shot noise of the optical signal: the shot noise is calculated according to $2e\overline{I}\Delta\nu$, where $\overline{I}$ is the average photodetector current. The average photodetector current can be found by $\overline{I} = \frac{e\overline{P_{\mathrm{in}}}}{h\nu}\eta$ and, thus, the shot noise of the optical signal is given by $2e^2\frac{P_{\mathrm{in}}\eta}{h\nu}\Delta\nu$.
4. Shot noise of the dark current to which we refer as simply the dark current noise is calculated according to $2ei_{\mathrm{d}}\Delta\nu$, where i_{d} is the dark current of the detector.

Next, we provide a quantitative estimate for each of the noise mechanisms, with the goal of estimating which of the noise mechanisms is relevant to our discussion. As a benchmark, we assume a photodiode area of 1 cm^2, bandwidth of 1 Hz, a solid angle of 2π, and room temperature operation. In addition, we assume $\phi_{\mathrm{B}} = 0.5$ and $\eta = 10^{-4}$ (typical values for this type of photodetector in the mid-IR[21]) .

We begin by estimating the background noise. To do so, one first needs to find the number of background photons, which can be estimated from blackbody radiation considerations. Thus, the number of background photons is given by

$$\int_{2\mu\mathrm{m}}^{2.5\mu\mathrm{m}} Q_{\mathrm{B}}(\lambda, T)\mathrm{d}\lambda = \int_{2\mu\mathrm{m}}^{2.5\mu\mathrm{m}} \frac{2\pi c}{\lambda^4\left(\exp\left(\frac{hc}{\lambda kT_{\mathrm{B}}}\right) - 1\right)}\mathrm{d}\lambda = 3.138 \times 10^{16}\left[\frac{\mathrm{photons}}{\mathrm{m}^2\cdot\mathrm{sec}}\right] = 3.138 \times 10^{12}\left[\frac{\mathrm{photons}}{\mathrm{cm}^2\cdot\mathrm{sec}}\right]$$

where we assumed an optical filter that is fully transparent between 2−2.5 μm and fully opaque elsewhere. The noise current power resulted from these photons is given by $\overline{i_{\mathrm{noise}}^2} = 2ei_{\mathrm{B}}\Delta\nu = 2e(Q_{\mathrm{B}}\eta e) = 1.609 \times 10^{-29}\ [A^2]$.

Now, we estimate the Johnson noise. Taking the load resistance to be 50Ω, the Johnson noise current power is $\frac{4kT_{\mathrm{B}}}{R_{\mathrm{L}}} = 3.31 \times 10^{-22}[A^2]$. For a larger load, this noise source could easily be reduced, albeit at the expense of operating at low frequencies.

Next, we would calculate the shot noise of the optical signal. It is given by $2e^2\frac{P}{h\nu}\eta = 5.8 \times 10^{-26}[A^2]$. Here, we have assumed a reasonable laser power of 1 mW.

Finally, we calculate the shot noise of the dark current. The dark current of our Schottky diode is given by[23]

$$I = SA^*T^2\ \exp\left(-\frac{e\phi_{\mathrm{B}}}{kT}\right)\left[\exp\left(\frac{eV_{\mathrm{a}}}{kT}\right) - 1\right] \tag{3}$$

where S is the detector area, A^* is the effective Richardson constant, and V_{a} is the applied voltage. Under reversed bias (the common way of operation), the dark current is $i_{\mathrm{d}} = SA^*T^2\ \exp\left(-\frac{e\phi_{\mathrm{B}}}{KT}\right)$. Assuming a realistic value of $A^* = 132\left[\frac{A}{\mathrm{cm}^2\cdot\mathrm{K}^2}\right]$, the noise that is generated due to dark current power is $\overline{i_{\mathrm{noise}}^2} = 2ei_{\mathrm{d}}\Delta\nu = 1.167 \times 10^{-20}\ [A^2]$.

From the above scenario, it appears that the dominant noise mechanism in IPE-based photodetectors is shot noise due to dark current. This should not be surprising, as it is well-known that the leakage current of Schottky diode is large in comparison to PN and PIN diodes because, unlike them, the Schottky diode is a majority carrier device. We now calculate what is the optimal Schottky barrier for achieving the highest SNR. Considering the shot noise due to dark current as the major noise source, the SNR can be approximated by

$$\mathrm{SNR} = \frac{\overline{i_{\mathrm{signal}}^2}}{\overline{i_{\mathrm{noise}}^2}} = \frac{\left(\frac{P_{\mathrm{in}}\eta}{h\nu}e\right)^2}{2eSA^*T^2\ \exp\left(-\frac{e\phi_{\mathrm{B}}}{kT}\right)} = \frac{\left(\frac{P_{\mathrm{in}}}{h\nu}eC\frac{(h\nu - \phi_{\mathrm{B}})^2}{h\nu}\right)^2}{2eSA^*T^2\ \exp\left(-\frac{e\phi_{\mathrm{B}}}{kT}\right)} \tag{4}$$

DOI: 10.1021/acsphotonics.7b00110
ACS Photonics 2017, 4, 1015−1020

We now take the derivative of the SNR with respect to ϕ_B and compared it to zero in order to find the optimal Schottky barrier.

$$\frac{d(SNR)}{d\phi_B} = 0$$

$$\phi_{B_{optimum}} = h\nu - \frac{4kT}{e} \quad (5)$$

This is a general result that allows the optimization of IPE-based photodetectors. The result holds for ideal diodes, assuming the dark current to be the dominant noise factor. In Figure 1 we plot the SNR of an IPE-based Schottky photodetector as a function of the Schottky barrier, ϕ_B, for the mid-IR wavelength of 2.15 μm, where all the above-mentioned noise mechanisms are included. Indeed, it can be seen that the highest SNR follows eq 5. For larger barrier values, the SNR is decreased because of the rapid drop in the signal (due to the rapid decrease in IPE efficiency), while for lower barrier values, the SNR is decreased because of the exponential increase in dark current. As can be seen, the optimum is relatively broad, and a decent SNR can be obtained even if the barrier height deviates slightly from the optimal value. Furthermore, one could observe that the decrease in SNR is moderate for barrier values which are lower than the optimum, whereas for values higher than the optimum, a rapid decrease in SNR is expected due to the rapid decrease in quantum efficiency. Thus, it might be a good practice to aim for having Schottky barriers, which are slightly lower than the optimum value.

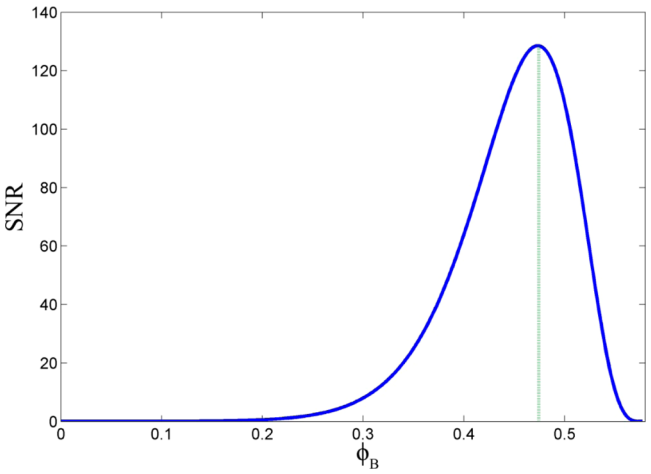

Figure 1. Calculated SNR as a function of the Schottky barrier (blue curve) for an input power of 30 μW and wavelength of 2.15 μm. All the above-mentioned noise mechanisms are included. The vertical green line is located at $\phi_B = h\nu - \frac{4kT}{e}$, denoting the peak of the SNR.

We note that the result of Figure 1 was calculated based on the assumption that the noise of the dark current is larger than the photonic shot noise. This assumption holds as long as the photon current is smaller than the diode leakage current (i.e., $\frac{P_{in}\eta}{h\nu}e \ll i_d$).

The above discussion is based on the assumption of an ideal Schottky diode. We now extend the discussion by considering a nonideal Schottky diode. In practice, a realistic Schottky diode can be modeled as an ideal diode with a shunt resistor in parallel (R_p) and a resistor in series (R_s), see Figure 2. The shunt resistance stems mostly from microscopic metal particles on the surface,[24] while the series resistor is originated from the finite conductivity between the Ohmic contact and the diode area.[23] For a typical diode the shunt resistor is few orders of magnitude higher than the series resistance ($R_p \gg R_s$). Typically, in reverse bias, the shunt current is about 2 orders of magnitude higher than the ideal leakage current of the diode.[24] As a result, the dark current is determined mostly by the shunt resistance.

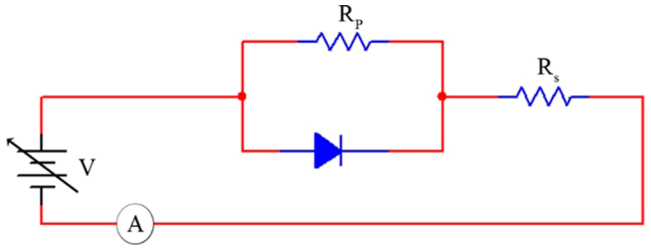

Figure 2. Equivalent circuit of a realistic Schottky diode. The R_p is the shunt resistance and R_s is the series resistance.

Considering this scenario, the SNR of such a detector is now given by

$$SNR = \frac{\overline{i^2_{signal}}}{\overline{i^2_{noise}}} = \frac{\left(\frac{P_{in}}{h\nu}eC\frac{(h\nu-\phi_B)^2}{h\nu}\right)^2}{2e\left(SA^*T^2\exp\left(-\frac{e\phi_B}{kT}\right) + G_pV_r + \frac{P_{in}}{h\nu}eC\frac{(h\nu-\phi_B)^2}{h\nu}\right)} \quad (6)$$

where G_p is the shunt conductivity and V_r is the applied reverse bias. Here, we have also included the photonic shot noise and thus the equation holds for a large parameter space, including cases where the detector area is small and the optical power is relatively large. For such a case, the optical shot noise is dominant.

Based on the equation above, we plot in Figure 3 the SNR against the Schottky barrier and the shunt resistance. To be compatible with the experimental results, which will be presented in the next section, we have chosen a small diode area of 0.785 μm^2 and a relatively low level of laser power (30 μW). For high shunt resistance, the dominant noise is originated from the leakage current of the diode. In such a case, the SNR is relatively high and two regimes can be easily observed, the low barrier regime, where the SNR is limited by a large leakage current, and the high barrier regime, where the SNR is limited by the rapid decrease in the IPE efficiency. As we reduce the shunt resistance, the shunt current becomes dominant, leading to a decrease in SNR. Furthermore, it also pulls the optimal SNR toward lower values of Schottky barrier. This is because up to some value, the reduction in Schottky barrier improves the IPE efficiency, while the noise barely increases as it is still dominant by the shunt current. Only when reducing the barrier beyond the point where the leakage current dominates the shunt current, one can observe a decrease in SNR.

Experimental Measurement of Mid-IR Schottky Photodetector. Following the above discussion, we now experimentally tackle the challenging task of mid-IR detection using uncooled IPE-based Schottky photodetector. Assuming an ideal diode, the Schottky barrier should be as close as possible to the optimal value of 0.475 eV to have the highest SNR at 2.15 μm. Furthermore, the SNR can be improved by adding optical structures which collect the signal from a large

DOI: 10.1021/acsphotonics.7b00110
ACS Photonics 2017, 4, 1015−1020

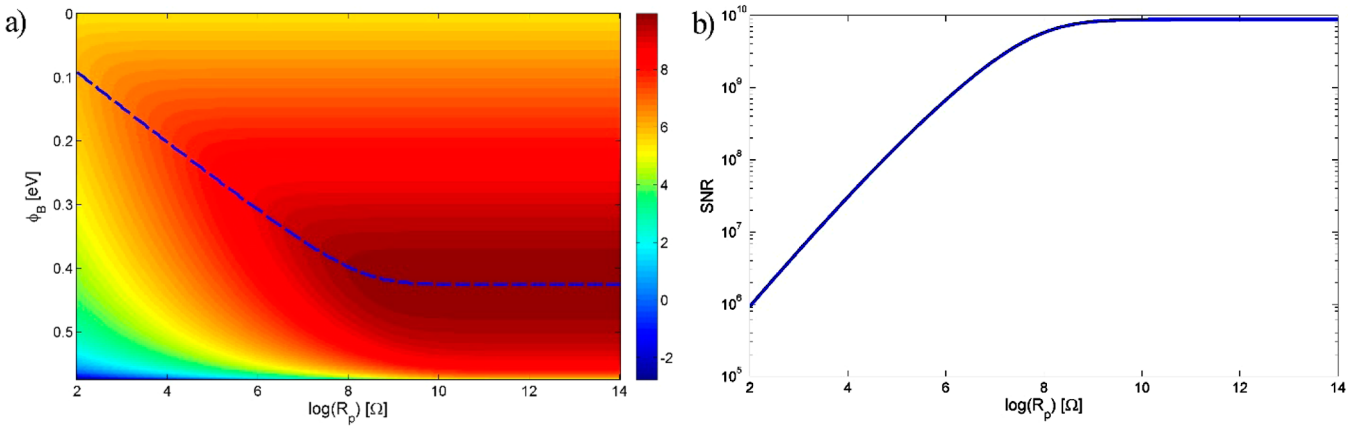

Figure 3. (a) SNR (log scale) calculation for a nonideal diode at the wavelength of 2.15 μm. Two regions can be observed: (1) high R_p (R_p > 100 MΩ), where the noise is dominated by the leakage current and the result converges toward that presented in Figure 1; and (2) low R_p, where the SNR is decreases and the optimum barrier tends toward lower values. The optimum barrier value as a function of the shunt resistance is denoted by the dashed blue line. In order to be compatible with experimental results to be presented in the next section, the Schottky diode area was chosen to be 0.78 μm^2. (b) Maximal SNR (log scale) vs shunt resistance.

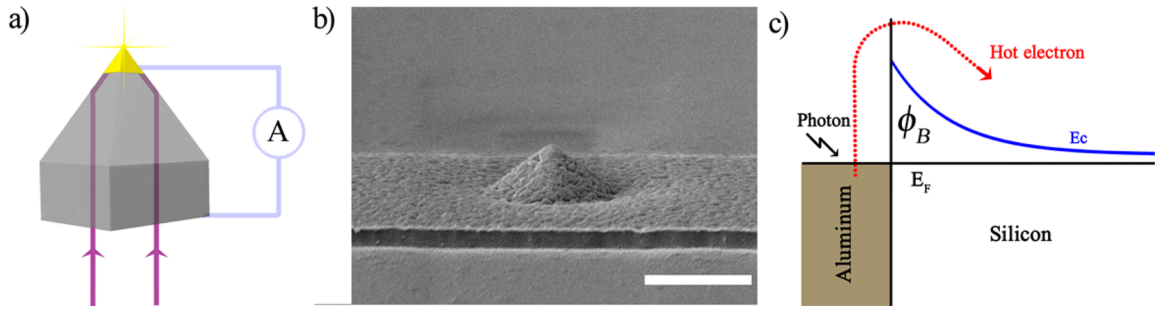

Figure 4. (a) Schematic drawing of the pyramidally shaped detection configuration. Light is incident from the backside of the silicon wafer and propagates toward the lower base of the pyramid, where it is guided toward its nanoscale apex. The active area of the photodetector is defined around the apex by adding the Schottky contact. (b) SEM micrograph showing a typical fabricated device. Scale bar is 1 μm. (c) Illustration of the internal photoemission process: photons (black arrow) are absorbed by the metal and excite hot electors (red). If the electron energy is higher than the Schottky barrier, it might be transported to the silicon and contribute to the photocurrent.

area and confine it to a smaller detector area. By doing so, one maintains high signal level, while reducing the noise. To cope with this goal, we have adopted the concept of pyramidally shaped silicon pillars, following the configuration which is described in details in ref 15.

Our photodetector is realized using a standard fabrication technique of anisotropic chemical wet etching in which pyramidally shaped devices are created in silicon by KOH etching. Implementation of this standard microelectronic fabrication technique provides the ability to fabricate silicon plasmonic photodetectors with a nanoscale pyramid apex and small active area without a need for "nanoscale" fabrication tools such as focused ion beam (FIB) or electron beam (Ebeam) lithography. The silicon pyramid acts as an efficient antenna, collecting the light from a large area and concentrating it into a small active pixel area, thus, providing high responsivity and in parallel low noise. A schematic drawing of our device is depicted in Figure 4. One should note that the silicon pyramids were passivated by a thick layer of SU8−3010 photoresist, which did cover the tip apex. The Schottky metal (aluminum) exists only in the tip apex.[15] This way, the dark current is minimized, allowing to obtain better SNR, which is particularly important for mid-IR operation.

Following the fabrication of the device, we have illuminated the structure with mid-IR light (tunable laser in the range of 2−2.5 μm, IPG Photonics) from the backside of the silicon wafer. Taking advantage of the high transparency of silicon in the mid-IR wavelength range, light is propagating through the wafer without noticeable absorption toward the bottom of the pyramid and is being guided effectively to the apex of the pyramid, where the active of the diode are located. Owing to its high refractive index of about 3.3, silicon offers high collection efficiency, preventing the light from escaping out of the pyramid as it is guided toward the apex, by supporting total internal reflection over a wide range of angles. The concept of operation is shown schematically in Figure 4. The effective diode area is 0.78 μm^2

Next, we performed electrical measurements at dark and under light illumination at various wavelengths ranging from ∼2 to ∼2.5 μm. The goal is to extract the Schottky barrier of the device, observe the SNR as a function of the incident wavelength of light and compare the measured results to the model presented earlier in the text.

The $I-V$ curves measured under illumination at various mid-IR wavelengths are present in Figure 5. By observing the obtained results, one can notice photodetection, even at the long wavelength of ∼2.5 μm. Considering the previously reported results in the near IR, such a device can essentially operate as a broad band detector, in the range of ∼1.1−2.5 μm.

DOI: 10.1021/acsphotonics.7b00110
ACS Photonics 2017, 4, 1015−1020

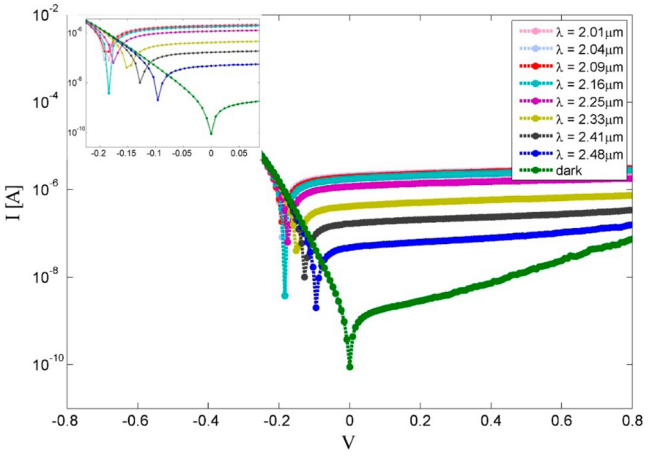

Figure 5. $I-V$ measurements of an internal photoemission photodetector under different wavelengths of excitation. The inset shows a zoom-in on the region of 0 V bias, which clearly indicates the lateral shift as a result of the photogenerated current.

Based on a set of measured $I-V$ curves, we have extracted the responsivity of the device at each wavelength (Figure 6a). Next, the Schottky barrier was found to be ϕ_B = 0.48 eV according to the Fowler model by plotting $\sqrt{Rh\nu} \propto h\nu - \phi_B$[23] (Figure 6b) and finding the intersection of $\sqrt{Rh\nu}$ with the y axis.

While responsivity and noise are important measures, one may ask what is the minimal optical power level that can be detected at a given electrical bandwidth. To cope with this question, we plot (Figure 7) the noise equivalent power (NEP, i.e the minimal power which can be detected in our system) as a function of wavelength. The experimental NEP values (green markers) were extracted from the measured responsivity ($R[A/W]$) and the measured dark current according to NEP = $\frac{\sqrt{2ei_d}}{R}$. For comparison, we also plot (solid blue line) the calculated NEP, derived using the shunt resistance as a single fitting parameter. The calculation is based on eq 6, with SNR = 1, ϕ_B = 0.48 eV and Fowler constant of C = 0.0029. These last two values are extracted from the measurements (Figure 6). Best fit

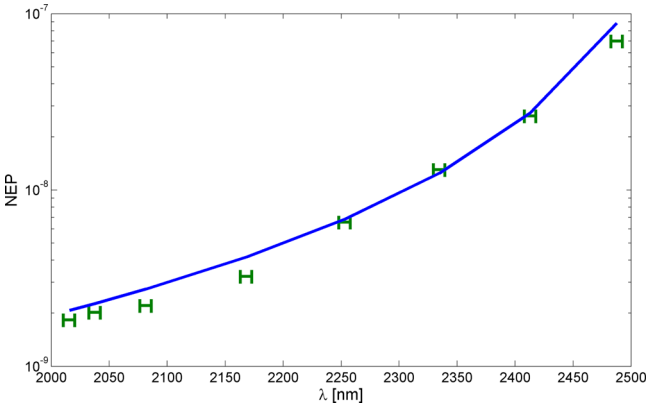

Figure 7. Measured (green) and calculated (solid blue line) NEP as a function of wavelength. Shunt resistance of 10 MΩ was assumed for the calculations.

was found for a shunt resistance of about 10 MΩ. As can be seen, the experimental results match very nicely to the previously discussed model (eq 6), assigning the SNR to be 1. The obtained results indicate that our device is capable of detecting optical signals in the nW regime. By controlling the Schottky barrier and by increasing the shunt resistance it should be possible to achieve NEP of $3.14 \times 10^{-10}\left[\frac{W}{\sqrt{\text{Hz}}}\right]$ at the wavelength of 2.15 μm. This NEP is obtained for the optimal Schottky barrier $\phi_B = h\nu - \frac{4kT}{e}$ with high shunt resistance (R_p > 6.1×10^{13} Ω). It should be mentioned that, while such NEP values are perhaps too high for night vision applications, they should be more than sufficient for laser driven applications.

CONCLUSIONS

In this work we have analyzed noise mechanisms of an IPE-based photodetector consisting of a Schottky contact between silicon and metal and demonstrated its capability of detecting light in the mid-infrared spectral band. Assuming an ideal diode, operating under realistic working conditions, the shot noise of the dark current was estimated to be the major noise mechanism. For such a scenario, we show that the optimal Schottky barrier in terms of maximizing the signal-to-noise ratio

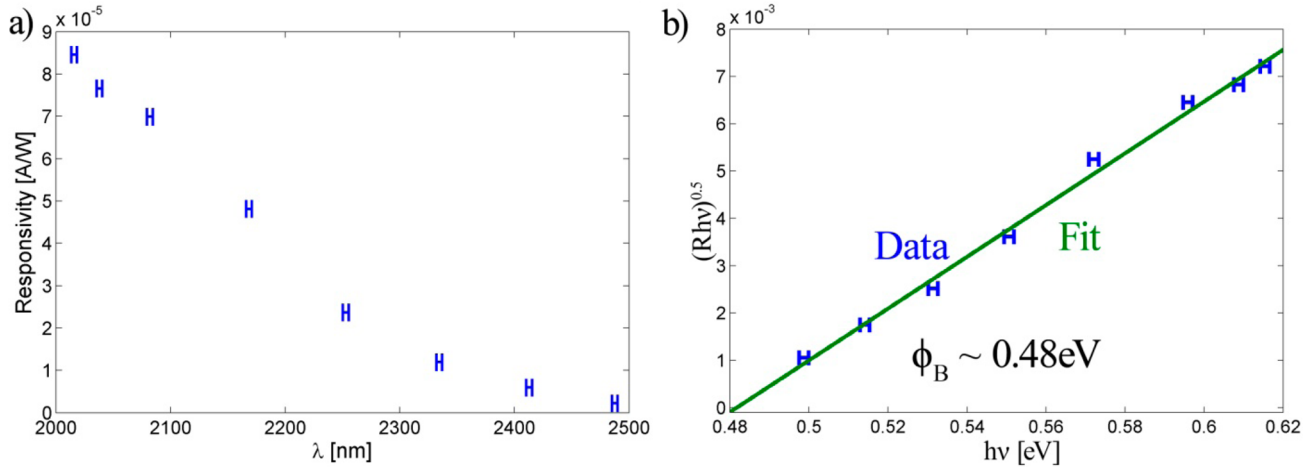

Figure 6. (a) Measured responsivity of the IPE-based device as a function of wavelength. The responsivity was found by extracting the current from several consecutive $I-V$ measurements performed under different optical power levels at a reverse bias of 0.8 V. (b) Applying the Fowler model to extract the Schottky barrier. The Barrier is found to be 0.48 eV.

DOI: 10.1021/acsphotonics.7b00110
ACS Photonics 2017, 4, 1015−1020

(SNR) is given by $\phi_B = h\nu - \frac{4kT}{e}$. This is a general result which is valid for an ideal photodetector based on IPE, as long as the dark current is the major noise factor. We also extend the model further to accommodate for nonideal diode, in which the shunt resistor is high and the noise is determined by shunt current. We show that for such a case the SNR is reduced and the Schottky barrier for optimal SNR should be lower. It should be noted that flicker noise was not included in the model because it was not observed experimentally in our system, even for frequencies as low as 1 Hz.

Following the presented model, we have fabricated and experimentally characterized an IPE-based Schottky detector in the mid-IR. The device was constructed in the form silicon pyramids, where the apex of the pyramid was covered by aluminum, creating a silicon-based Schottky photodetector with a Schottky barrier of 0.48 eV. Our measurements indicate that the photodetector has a wide spectral response, up to 2.48 μm at room temperature. The experimental results are compared against the model, showing good agreement. Specifically, noise equivalent power (NEP), are in the range of $10^{-8}\left[\frac{W}{\sqrt{Hz}}\right]$ and even below.

Based on the model and the experimental results, we now provide guidelines for optimizing an IPE-based Schottky photodetector. Briefly, the Shunt resistance should be as high as possible, while the Schottky barrier needs to be optimized for the specific wavelength of operation. This choice of parameters, together with approaches for enhancing the IPE efficiency, such as roughness engineering and high localization of the electromagnetic mode, are instrumental for achieving high quality photodetectors, in particular, for the mid-IR, where the SNR is inherently low.

Finally, while the model was applied here for the mid-IR spectral regime, it can be easily applied to other spectral bands as well. Furthermore, our device can be integrated with other photodetectors, for example, using wafer bonding techniques or by the realization of our detector in the backside of a visible band silicon photodetector. Such an approach will allow efficient photodetection of multiple spectral bands (e.g., visible and IR). The demonstration of such an integrated approach remains for future work.

AUTHOR INFORMATION

Corresponding Author

*E-mail: ulevy@mail.huji.ac.il.

ORCID

Meir Grajower: 0000-0003-4973-1800

Uriel Levy: 0000-0002-5918-1876

Notes

The authors declare no competing financial interest.

ACKNOWLEDGMENTS

The research was supported by the Israel-US BSF Program and by the PETACLOUD consortium.

REFERENCES

(1) Michel, J.; Liu, J.; Kimerling, L. C. High-Performance Ge-on-Si Photodetectors. *Nat. Photonics* **2010**, *4*, 527−534.

(2) Roelkens, G.; Van Thourhout, D.; Baets, R.; Nötzel, R.; Smit, M. Laser Emission and Photodetection in an InP/InGaAsP Layer Integrated on and Coupled to a Silicon-on-Insulator Waveguide Circuit. *Opt. Express* **2006**, *14*, 8154.

(3) Ban, V. S.; Erickson, G.; Mason, S.; Woodruff, K.; Gasparian, G.; Olsen, G. H. Room-Temperature Detectors For 800−2600 nm Based On InGaAsP Alloys. *Proc. SPIE* **1989**, 151−164.

(4) Semiconductor Photodetectors | RMT Ltd; http://www.rmtltd.ru/applications/photodetectors/semicond.php.

(5) Downs, C.; Vandervelde, T. Progress in Infrared Photodetectors Since 2000. *Sensors* **2013**, *13*, 5054−5098.

(6) Rogalski, A. Infrared Detectors: An Overview. *Infrared Phys. Technol.* **2002**, *43*, 187−210.

(7) Dat, R. Advances in Infrared Detector Array Technology. *Optoelectronics - Advanced Materials and Devices*: InTech, 2013.

(8) Chang, C.; Li, H.; Huang, S. H.; Cheng, H. H.; Sun, G.; Soref, R. A. Sn-Based Ge/Ge $_{0.975}$ Sn $_{0.025}$ /Ge P-I-N Photodetector Operated with Back-Side Illumination. *Appl. Phys. Lett.* **2016**, *108*, 151101.

(9) Pham, T.; Du, W.; Tran, H.; Margetis, J.; Tolle, J.; Sun, G.; Soref, R. A.; Naseem, H. A.; Li, B.; Yu, S.-Q. Systematic Study of Si-Based GeSn Photodiodes with 26 Mm Detector Cutoff for Short-Wave Infrared Detection. *Opt. Express* **2016**, *24*, 4519.

(10) Goykhman, I.; Desiatov, B.; Khurgin, J.; Shappir, J.; Levy, U. Waveguide Based Compact Silicon Schottky Photodetector with Enhanced Responsivity in the Telecom Spectral Band. *Opt. Express* **2012**, *20*, 28594.

(11) Ishi, T.; Fujikata, J.; Marita, K.; Baba, T.; Ohashi, K. Si Nano-Photodiode with a Surface Plasmon Antenna. *Jpn. J. Appl. Phys.* **2005**, *44*, L364−L366.

(12) Knight, M. W.; Sobhani, H.; Nordlander, P.; Halas, N. J. Photodetection with Active Optical Antennas. *Science* **2011**, *332*, 702−704.

(13) Akbari, A.; Tait, R. N.; Berini, P. Surface Plasmon Waveguide Schottky Detector. *Opt. Express* **2010**, *18*, 8505.

(14) Muehlbrandt, S.; Melikyan, A.; Harter, T.; Köhnle, K.; Muslija, A.; Vincze, P.; Wolf, S.; Jakobs, P.; Fedoryshyn, Y.; Freude, W.; Leuthold, J.; Koos, C.; Kohl, M. Silicon-Plasmonic Internal-Photoemission Detector for 40 Gbit/s Data Reception. *Optica* **2016**, *3*, 741.

(15) Desiatov, B.; Goykhman, I.; Mazurski, N.; Shappir, J.; Khurgin, J. B.; Levy, U. Plasmonic Enhanced Silicon Pyramids for Internal Photoemission Schottky Detectors in the near-Infrared Regime. *Optica* **2015**, *2*, 335.

(16) Goykhman, I.; Desiatov, B.; Khurgin, J.; Shappir, J.; Levy, U. Locally Oxidized Silicon Surface-Plasmon Schottky Detector for Telecom Regime. *Nano Lett.* **2011**, *11*, 2219−2224.

(17) Mooney, J. M.; Silverman, J. The Theory of Hot-Electron Photoemission in Schottky-Barrier IR Detectors. *IEEE Trans. Electron Devices* **1985**, *32*, 33−39.

(18) Akbari, A.; Berini, P. Schottky Contact Surface-Plasmon Detector Integrated with an Asymmetric Metal Stripe Waveguide. *Appl. Phys. Lett.* **2009**, *95*, 21104.

(19) Scales, C.; Berini, P. Thin-Film Schottky Barrier Photodetector Models. *IEEE J. Quantum Electron.* **2010**, *46*, 633−643.

(20) Fowler, R. H. The Analysis of Photoelectric Sensitivity Curves for Clean Metals at Various Temperatures. *Phys. Rev.* **1931**, *38*, 45−56.

(21) Goykhman, I.; Desiatov, B.; Shappir, J.; Khurgin, J. B.; Levy, U. Model for Quantum Efficiency of Guided Mode Plasmonic Enhanced Silicon Schottky Detectors. *arXiv:1401.2624* **2014**, n/a.

(22) Yariv, A.; Yeh, P.; Yariv, A. *Photonics: Optical Electronics in Modern Communications*; Oxford University Press, 2007.

(23) Sze, S. M.; Ng, K. K. *Physics of Semiconductor Devices*; Wiley-Interscience, 2007.

(24) Werner, J. H. Schottky Barrier and Pn-junctionI/V Plots ? Small Signal Evaluation. *Appl. Phys. A: Solids Surf.* **1988**, *47*, 291−300.

DOI: 10.1021/acsphotonics.7b00110
ACS Photonics 2017, 4, 1015−1020